AMERICAN SOCIETY FOR MICROBIOLOGY | Antimicrobial Agents and Chemotherapy®

ANTIVIRAL AGENTS

In Vitro Selection of Remdesivir-Resistant SARS-CoV-2 Demonstrates High Barrier to Resistance

Liva Checkmahomed,[a] Julie Carbonneau,[a] Venice Du Pont,[b] Nicholas C. Riola,[b] Jason K. Perry,[b] Jiani Li,[b] Bastien Paré,[c] Shawn M. Simpson,[c] Martin A. Smith,[c] Danielle P. Porter,[b] Guy Boivin[a]

[a]CHU de Quebec Hospital and Laval University, Quebec City, Quebec, Canada
[b]Gilead Sciences, Foster City, California, USA
[c]Ste-Justine Hospital and University of Montréal, Montréal, Quebec, Canada

ABSTRACT *In vitro* selection of remdesivir-resistant severe acute respiratory syndrome coronavirus 2 (SARS-CoV-2) revealed the emergence of a V166L substitution, located outside of the polymerase active site of the Nsp12 protein, after 9 passages of a single lineage. V166L remained the only Nsp12 substitution after 17 passages (10 μM remdesivir), conferring a 2.3-fold increase in 50% effective concentration (EC_{50}). When V166L was introduced into a recombinant SARS-CoV-2 virus, a 1.5-fold increase in EC_{50} was observed, indicating a high *in vitro* barrier to remdesivir resistance.

KEYWORDS SARS-CoV-2, Nsp12 polymerase, remdesivir, resistance

Remdesivir (RDV; VEKLURY), a nucleotide prodrug inhibitor of the severe acute respiratory syndrome coronavirus 2 (SARS-CoV-2) RNA-dependent RNA polymerase (Nsp12), is one of the few approved antiviral drugs for the treatment of coronavirus 19 (COVID-19) (1, 2). Characterization of clinical resistance development to this compound is currently in progress. So far, *in vitro* resistance to this antiviral has been rarely reported in SARS-CoV-2 and other viruses (3–5).

In this study, we sought to select an RDV-resistant virus by serial passaging of a wild-type (WT) SARS-CoV-2 Canadian isolate in the presence of increasing concentrations of RDV in cell culture.

The V166L substitution located in the Nsp12 protein was detected after 9 passages reaching 6 μM RDV (Table 1). This mutation was not present in the WT virus passaged in parallel in the absence of drug. The same substitution was detected at passages 11 and 17 (in the presence of 8 and 10 μM RDV, respectively) of a single lineage. Deep sequencing revealed no other emergent Nsp12 mutations, but substitutions were detected in other genes (F184V in nsp6, Q992H and S1142L in Spike, P10S in ORF10) at passages 9 and 17, which were not present in strains passaged in the absence of RDV (GenBank accession numbers ON072482-ON072487). Further passages beyond 10 μM RDV resulted in tiny plaques or absence of cytopathic effects. Virus isolates from passages 6, 10, and 17 exhibited a 3.9-, 2.7-, and 2.3-fold reduced susceptibility to RDV compared to the WT isolate using a plaque reduction assay in Vero E6 cells. The V166L substitution remained the only Nsp12 mutation that emerged in the presence of RDV throughout the resistance selection process.

When introduced into a SARS-CoV-2-Nluc recombinant WT WA1 virus, the Nsp12 P323L substitution (present at baseline in the passaged virus SARS-CoV-2/Québec/21697/2020 and predominant in currently circulating strains of SARS-CoV-2) plus the V166L Nsp12 substitution (identified in the RDV-selected virus population) minimally increased the RDV 50% effective concentration (EC_{50}) value by 1.5-fold relative to the WT reference virus using a luciferase assay (EC_{50} Nsp12-V166L/P323L = 0.09 $\pm$ 0.01 μM; Nsp12-WT = 0.06 $\pm$ 0.01 μM; Table 2 and Fig. 1A). To determine the effect of the resistance-selected Nsp12 substitution V166L on replication kinetics, viral replication assays were performed. SARS-CoV-2-Nluc expressing the

Address correspondence to Guy Boivin, Guy.Boivin@crchudequebec.ulaval.ca.

The authors declare a conflict of interest. 5 of the authors work at Gilead Sciences.

Received 4 February 2022
Returned for modification 3 March 2022
Accepted 26 May 2022
Published 16 June 2022

TABLE 1 EC_{50} values and nonsynonymous emergent substitutions present in SARS-CoV-2/Québec/21697/2020 after serial passaging in the presence of RDV[a]

Passage no.[b]	RDV concentration (μM)	Average RDV EC_{50} ± SD (μM)[c]	EC_{50} fold change from wild type	Nsp12 emergent substitutions detected (% of reads)
0 (WT; Québec)		1.35 ± 1.00[d]	1.0	
4	4	ND	ND	None
9	6	5.27[e]	3.9	V166L (83%)
11	8	3.75[e]	2.7	V166L (ND)
17	10	3.08 ± 0.95[d]	2.3	V166L (97%)

[a]EC_{50}, 50% effective concentration; MOI, multiplicity of infection; ND, not determined; RDV, remdesivir; SARS-CoV-2, severe acute respiratory syndrome coronavirus 2; WT, wild type.
[b]A single lineage was passaged in the presence of gradually increasing concentrations of RDV.
[c]RDV susceptibilities of the selected virus populations from passages 9, 11, and 17 were determined by plaque reduction assay in Vero E6 cells infected with an MOI of 0.001.
[d]Data from 3 independent experiments.
[e]Data from single experiment.

Nsp12-P323L substitution exhibited similar replication kinetics to Nsp12-WT reporter virus. However, the RDV-selected Nsp12 substitution Nsp12-V166L/P323L demonstrated significant reduction in titer for the 72- and 96-h time points compared to Nsp12-WT (Fig. 1B).

A structural analysis identified residue 166 as located outside of the polymerase active site (Fig. 2), but contacts residues in the active site Motifs A and D. Modeling suggests V166L provides only a modest perturbation of Motif D; therefore, any impact from this substitution on RDV potency is suspected to be indirect. Furthermore, an extensive search in sequencing databases in April 2022 identified the V166L substitution in 0.003% (332/10236858) of SARS-CoV-2 sequences reported.

RDV is a broad-spectrum RNA polymerase inhibitor of several viral families including *Coronaviridae*, *Filoviridae*, *Pneumoviridae*, and *Paramyxoviridae* (6, 7). Furthermore, it is the first antiviral approved by the FDA for the treatment of hospitalized and nonhospitalized cases of COVID-19. RDV resistance has been rarely documented (3–5). Passaging SARS-CoV-2 *in vitro* in the presence of increasing concentrations of RDV selected a single substitution (V166L) in the viral polymerase Nsp12 protein, which was associated with a minimal 1.5-fold increase in the RDV EC_{50} value after introduction into a recombinant virus. The low level of resistance was similar between the recombinant V166L virus and the various passages of the drug-selected strains (i.e., 1.5-fold and 2.3-fold to 3.9-fold). A comparison of growth kinetics to the reference strain (WA1) revealed that introduction of the V166L substitution decreased viral fitness. Whole genome sequencing of the serially passaged viral populations revealed additional substitutions in Nsp6, Spike, and ORF10, which may have arisen as compensatory substitutions to alleviate potential strains caused by the V166L substitution on replication. It is possible that these additional changes in the selected virus population outside of Nsp12 or differences in the assays used to evaluate RDV antiviral activity may have contributed to these slight differences in fold change and/or replication kinetics observed.

Recently, in an immunocompromised patient with prolonged SARS-CoV-2 shedding, the V166L substitution in Nsp12 was observed after treatment with two 10-day courses of RDV and two units of convalescent plasma (unknown phenotype) (8). The population carrying this substitution was eventually outcompeted by virus with substitutions and deletions within

TABLE 2 RDV potencies against recombinant SARS-CoV-2-Nluc WA1 and Nsp12 substituted viruses

Nsp12 substitution	Mean EC_{50} ± SD (μM)[a]	Mean EC_{50} fold change ± SD from WT[b]
WT (WA1)	0.06 ± 0.01	1.0
P323L	0.07 ± 0.02	1.2 ± 0.04
V166L/P323L	0.09 ± 0.01	1.5 ± 0.29

[a]RDV susceptibilities of recombinant SARS-CoV-2-Nluc WA1 with indicated substitutions were determined by relative luciferase units in A549-hACE2 cells infected at MOI 0.05. Data represent the mean and SD from 2 independent experiments.
[b]Fold change was calculated for each independent experiment and mean fold change ± SD was calculated with these values.

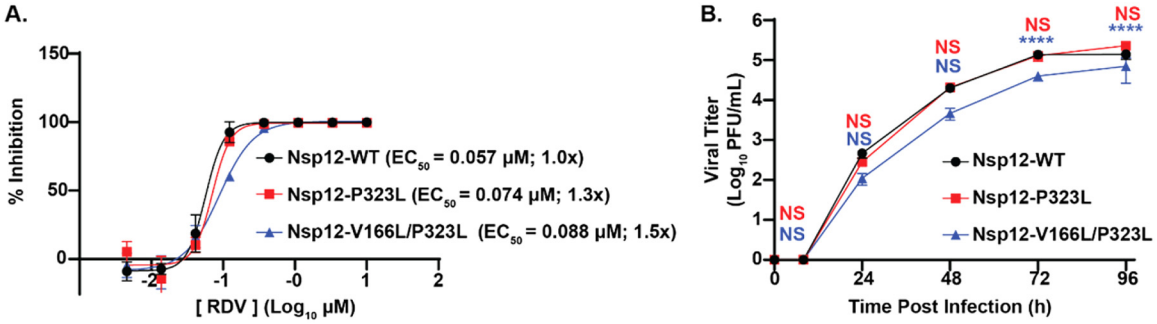

FIG 1 Antiviral assays and replication of severe acute respiratory syndrome coronavirus 2 (SARS-CoV-2)-Nluc viruses. (A) Activity of remdesivir (RDV) against SARS-CoV-2-Nluc WA1 expressing Nsp12-WT, Nsp12-P323L, and RDV-selected substitution Nsp12-V166L/P323L in A549-hACE2 cells infected at MOI 0.05. Dose-response curves are based on at least 2 independent experiments with two technical replicates each and fit based on a nonlinear regression model using GraphPad Prism 8. (B) Viral replication kinetics of SARS-CoV-2-Nluc WA1 expressing Nsp12-WT, Nsp12-P323L, and RDV-selected substitution Nsp12-V166L/P323L in A549-hACE2-TMPRSS2 cells infected at multiplicity of infection of 0.01. Viral titer for each indicated time point was determined by plaque-reduction assays performed in Vero-TMPRSS2 cells in triplicate. EC_{50}, 50% effective concentration. Statistical analysis was performed by two-way ANOVA with Tukey's *post hoc* comparison tests. (NS, not significant; ****, $P \leq 0.0001$).

spike and contained a WT Nsp12 after a third course of RDV treatment in conjunction with an additional unit of convalescent plasma. This case study demonstrates the instability of the V166L substitution in a treatment setting as well as complements our finding that there is a fitness cost associated with V166L such that the virus has a propensity to revert to WT. Additionally, *in vitro* resistance selection experiments conducted by serially passaging SARS-CoV-2 in the presence of GS-441524 resulted in amino acid change Nsp12-V166A coselected with Nsp12 substitutions N198S, S759A, and C799F after 13 passages (5). Based on its structural location in Nsp12, V166A alone may only cause mild perturbation of Motif D and may require additional substitutions to confer the 10-fold reduced susceptibility observed in lineage 1 of the GS-441524-selected virus population (5).

In another case report, virus isolated from an immunocompromised patient who received 10 days of RDV contained the E802D substitution in Nsp12 (9). Recently, the E802D substitution was selected after serial passage of SARS-CoV-2 in the presence of RDV *in vitro* and conferred a 2.5-fold increase in EC_{50} value. Notably, this substitution was also associated with a fitness cost (4).

Additional *in vitro* studies have been conducted with coronaviruses that identified substitutions associated with resistance to RDV. Passage of the murine hepatitis virus in the presence of GS-441524 (the parent nucleoside analog of RDV) selected two substitutions

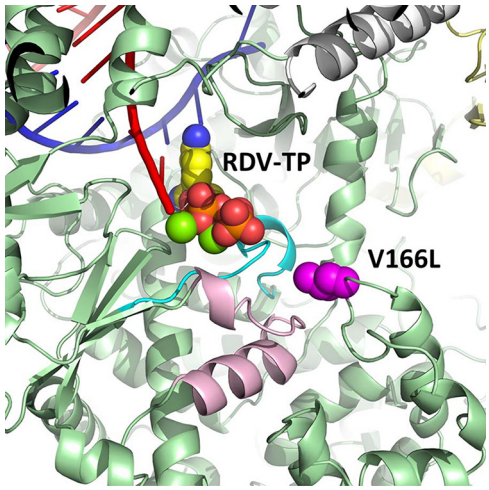

FIG 2 Model of preincorporated RDV triphosphate (RDV-TP) with a V166L substitution (magenta) in SARS-CoV-2 Nsp12 (green). V166L is outside of the active site but contacts Motif A (cyan) and Motif D (pink) residues. Nsp7 and Nsp8 are visible in white and yellow, respectively. The nascent RNA strand is in red and the template strand is in blue. The software Maestro, Prime, and Macromodel, within the Schrödinger software suite, were used to perform structural analysis.

(F476L and V553L) after 23 passages that conferred low-level (5.6-fold) resistance to RDV. Introduction of the orthologous substitutions into SARS-CoV resulted in 6-fold reduced susceptibility to RDV *in vitro* in addition to attenuated pathogenesis in a mouse model (3).

The high number of passages reached at which only a single V166L substitution emerged and the minimal change in susceptibility to RDV associated with this substitution in addition to its fitness cost highlight the high genetic barrier of resistance for RDV.

The SARS-CoV-2/Québec/21697/2020 strain was used for the resistance selection experiments described in this study. This strain of SARS-CoV-2 contains the D614G substitution in the spike protein as well as A250V and P323L substitutions in the Nsp12 polymerase when compared with the lineage A WA1 reference strain. The virus was isolated from a clinical sample at CHUL, Québec City, Canada and was passaged as a single lineage in Vero E6 cells initially in the presence of 1 μM RDV followed by increasing the drug concentration until clear virally induced cytopathic effects were noted. A control virus was passaged concomitantly in the absence of drug during all the selection procedure. At specified RDV concentrations, EC_{50} values were determined by a plaque reduction assay (10), and the Nsp12 genotype was determined by PCR amplification followed by Sanger sequencing. In addition, complete sequences of viral genomes at selected passages were determined using a published SARS-CoV-2 protocol (11) and MinION flowcells on a GridION X5 sequencer (Oxford Nanopore Technologies). Internally developed software at Gilead Sciences was used to process and align Oxford Nanopore deep sequencing data via a multistep method. Oxford Nanopore deep sequencing reads were filtered to exclude human RNA transcripts and then aligned to Wuhan-Hu-1 (NC_045512) using minimap2 v2.17. Nucleotide variants were reported per genome position at frequency $\geq$15%, excluding any variants overlapping with primers, average phred score $<$10, forward strand ratio $<$0.1 or $>$0.9, and read depth $<$50.

The P323L and emergent Nsp12 substitutions were introduced into a recombinant WA1 (2019-nCoV/USA_WA1/2020; GenBank accession number QHU79204) SARS-CoV-2-Nano luciferase (Nluc) reporter virus. The reverse genetics system was kindly provided by the University of Texas Medical Branch (Galveston, TX), and the procedures required to assemble and produce SARS-CoV-2 infectious strains have been previously described in detail by Xie et al. (12). Antiviral activity (EC_{50} value) of RDV against SARS-CoV-2-Nluc was evaluated with a luciferase assay as reported (13) with some modifications (14).

To determine the impact of substitutions on replication kinetics, A549-hACE2 cells expressing TMPRSS2 (InvivoGen, San Diego, CA) were seeded into 48-well plates at 5×10^4 cells/well with media containing 10% FBS, 0.5 μg/mL puromycin, and 100 μg/mL hygromycin. On the following day, cells were adsorbed with either WT or Nsp12-substituted SARS-CoV-2-Nluc viruses at MOI 0.01 for 30 min on a rocker at 37°C with 5% CO_2. The inoculum was then removed, and cells were washed three times with prewarmed PBS and replaced with DMEM containing 2% FBS. Supernatants were harvested at times 0, 8, 24, 48, 72, and 96 h postinfection. Titers were determined for each time point by plaque assay (14). The data represent three individual experiments for each time point for each recombinant virus. Two-way ANOVA with Tukey's *post hoc* multiple comparisons tests were used to assess statistical differences between samples using the GraphPad Prism 8 software package.

A structural model of the SARS-CoV-2 polymerase complex with preincorporated RDV triphosphate (RDV-TP) was generated from the cryo-EM structure 6XEZ (15) as described elsewhere (16). V166 was substituted to an L, and all residues within 5 Å of this residue were conformationally sampled and minimized for both WT and V166L, using Maestro, Prime, and Macromodel, within the Schrödinger software suite (17).

A total of n = 10,236,858 genome sequences were deposited in GISAID database as of April 21, 2022. The tabulated amino acid substitutions from Wuhan-Hu-1 reference sequence (NC_045512) for each SARS-CoV-2 sequence (variant surveillance package) were downloaded through GISAID web portal (https://www.gisaid.org/) to assess the prevalence of the mutation.

REFERENCES

1. Beigel JH, Tomashek KM, Dodd LE, Mehta AK, Zingman BS, Kalil AC, Hohmann E, Chu HY, Luetkemeyer A, Kline S, Lopez de Castilla D, Finberg RW, Dierberg K, Tapson V, Hsieh L, Patterson TF, Paredes R, Sweeney DA, Short WR, Touloumi G, Lye DC, Ohmagari N, Oh MD, Ruiz-Palacios GM, Benfield T, Fatkenheuer G,

Kortepeter MG, Atmar RL, Creech CB, Lundgren J, Babiker AG, Pett S, Neaton JD, Burgess TH, Bonnett T, Green M, Makowski M, Osinusi A, Nayak S, Lane HC, ACTT-1 Study Group Members. 2020. Remdesivir for the treatment of COVID-19–final report. N Engl J Med 383:1813–1826. https://doi.org/10.1056/NEJMoa2007764.

2. Hall MD, Anderson JM, Anderson A, Baker D, Bradner J, Brimacombe KR, Campbell EA, Corbett KS, Carter K, Cherry S, Chiang L, Cihlar T, de Wit E, Denison M, Disney M, Fletcher CV, Ford-Scheimer SL, Gotte M, Grossman AC, Hayden FG, Hazuda DJ, Lanteri CA, Marston H, Mesecar AD, Moore S, Nwankwo JO, O'Rear J, Painter G, Singh Saikatendu K, Schiffer CA, Sheahan TP, Shi PY, Smyth HD, Sofia MJ, Weetall M, Weller SK, Whitley R, Fauci AS, Austin CP, Collins FS, Conley AJ, Davis MI. 2021. Report of the National Institutes of Health SARS-CoV-2 Antiviral Therapeutics Summit. J Infect Dis 224:S1–S21. https://doi.org/10.1093/infdis/jiab305.
3. Agostini ML, Andres EL, Sims AC, Graham RL, Sheahan TP, Lu X, Smith EC, Case JB, Feng JY, Jordan R, Ray AS, Cihlar T, Siegel D, Mackman RL, Clarke MO, Baric RS, Denison MR. 2018. Coronavirus susceptibility to the antiviral remdesivir (GS-5734) is mediated by the viral polymerase and the proofreading exoribonuclease. mBio 9:e00221-18. https://doi.org/10.1128/mBio.00221-18.
4. Szemiel AM, Merits A, Orton RJ, MacLean OA, Pinto RM, Wickenhagen A, Lieber G, Turnbull ML, Wang S, Furnon W, Suarez NM, Mair D, da Silva Filipe A, Willett BJ, Wilson SJ, Patel AH, Thomson EC, Palmarini M, Kohl A, Stewart ME. 2021. In vitro selection of Remdesivir resistance suggests evolutionary predictability of SARS-CoV-2. PLoS Pathog 17:e1009929. https://doi.org/10.1371/journal.ppat.1009929.
5. Stevens LJ, Pruijssers AJ, Lee HW, Gordon CJ, Tchesnokov EP, Gribble J, George AS, Hughes TM, Lu X, Li J, Perry JK, Porter DP, Cihlar T, Sheahan TP, Baric RS, Götte M, Denison MR. 2022. Distinct genetic determinants and mechanisms of SARS-CoV-2 resistance to remdesivir. BioRxiv. https://doi.org/10.1101/2022.01.25.477724.
6. Xu Y, Barauskas O, Kim C, Babusis D, Murakami E, Kornyeyev D, Lee G, Stepan G, Perron M, Bannister R, Schultz BE, Sakowicz R, Porter D, Cihlar T, Feng JY. 2021. Off-target in vitro profiling demonstrates that remdesivir is a highly selective antiviral agent. Antimicrob Agents Chemother 65:e02237-20. https://doi.org/10.1128/AAC.02237-20.
7. Lo MK, Jordan R, Arvey A, Sudhamsu J, Shrivastava-Ranjan P, Hotard AL, Flint M, McMullan LK, Siegel D, Clarke MO, Mackman RL, Hui HC, Perron M, Ray AS, Cihlar T, Nichol ST, Spiropoulou CF. 2017. GS-5734 and its parent nucleoside analog inhibit Filo-, Pneumo-, and Paramyxoviruses. Sci Rep 7:43395. https://doi.org/10.1038/srep43395.
8. Kemp SA, Collier DA, Datir RP, Ferreira I, Gayed S, Jahun A, Hosmillo M, Rees-Spear C, Mlcochova P, Lumb IU, Roberts DJ, Chandra A, Temperton N, CITIID-NIHR BioResource COVID-19 Collaboration, COVID-19 Genomics UK (COG-UK) Consortium, Sharrocks K, Blane E, Modis Y, Leigh KE, Briggs JAG, van Gils MJ, Smith KGC, Bradley JR, Smith C, Doffinger R, Ceron-Gutierrez L, Barcenas-Morales G, Pollock DD, Goldstein RA, Smielewska A, Skittrall JP, Gouliouris T, Goodfellow IG, Gkrania-Klotsas E, Illingworth CJR, McCoy LE, Gupta RK. 2021. SARS-CoV-2 evolution during treatment of chronic infection. Nature 592:277–282. https://doi.org/10.1038/s41586-021-03291-y.
9. Gandhi S, Klein J, Robertson AJ, Pena-Hernandez MA, Lin MJ, Roychoudhury P, Lu P, Fournier J, Ferguson D, Mohamed Bakhash SAK, Catherine Muenker M, Srivathsan A, Wunder EA, Jr, Kerantzas N, Wang W, Lindenbach B, Pyle A, Wilen CB, Ogbuagu O, Greninger AL, Iwasaki A, Schulz WL, Ko AI. 2022. De novo emergence of a remdesivir resistance mutation during treatment of persistent SARS-CoV-2 infection in an immunocompromised patient: a case report. Nat Commun 13:1547. https://doi.org/10.1038/s41467-022-29104-y.
10. Niesor EJ, Boivin G, Rheaume E, Shi R, Lavoie V, Goyette N, Picard ME, Perez A, Laghrissi-Thode F, Tardif JC. 2021. Inhibition of the 3CL protease and SARS-CoV-2 replication by dalcetrapib. ACS Omega 6:16584–16591. https://doi.org/10.1021/acsomega.1c01797.
11. Freed NE, Vlkova M, Faisal MB, Silander OK. 2020. Rapid and inexpensive whole-genome sequencing of SARS-CoV-2 using 1200 bp tiled amplicons and Oxford Nanopore Rapid Barcoding. Biol Methods Protoc 5:bpaa014. https://doi.org/10.1093/biomethods/bpaa014.
12. Xie X, Muruato A, Lokugamage KG, Narayanan K, Zhang X, Zou J, Liu J, Schindewolf C, Bopp NE, Aguilar PV, Plante KS, Weaver SC, Makino S, LeDuc JW, Menachery VD, Shi PY. 2020. An infectious cDNA clone of SARS-CoV-2. Cell Host Microbe 27:841–848.e3. https://doi.org/10.1016/j.chom.2020.04.004.
13. Xie X, Muruato AE, Zhang X, Lokugamage KG, Fontes-Garfias CR, Zou J, Liu J, Ren P, Balakrishnan M, Cihlar T, Tseng CK, Makino S, Menachery VD, Bilello JP, Shi PY. 2020. A nanoluciferase SARS-CoV-2 for rapid neutralization testing and screening of anti-infective drugs for COVID-19. Nat Commun 11:5214. https://doi.org/10.1038/s41467-020-19055-7.
14. Pitts J, Li J, Perry JK, Du Pont V, Riola N, Rodriguez L, Lu X, Kurhade C, Xie X, Camus G, Manhas S, Martin R, Shi PY, Cihlar T, Porter DP, Mo H, Maiorova E, Bilello JP. 2022. Remdesivir and GS-441524 retain antiviral activity against Delta, Omicron, and other emergent SARS-CoV-2 variants. BioRxiv. https://doi.org/10.1101/2022.02.09.479840.
15. Chen J, Malone B, Llewellyn E, Grasso M, Shelton PMM, Olinares PDB, Maruthi K, Eng ET, Vatandaslar H, Chait BT, Kapoor TM, Darst SA, Campbell EA. 2020. Structural basis for helicase-polymerase coupling in the SARS-CoV-2 replication-transcription complex. Cell 182:1560–1573.e13. https://doi.org/10.1016/j.cell.2020.07.033.
16. Gordon CJ, Lee HW, Tchesnokov EP, Perry JK, Feng JY, Bilello JP, Porter DP, Gotte M. 2021. Efficient incorporation and template-dependent polymerase inhibition are major determinants for the broad-spectrum antiviral activity of remdesivir. J Biol Chem 298:101529.
17. Schrödinger. 2021. Release 2021-3 SSR. Schrödinger, LLC, New York, NY. https://www.schrodinger.com/releases/release-2021-3.